G PROTEIN SIGNALING

Copyright © 2018 The Authors, some rights reserved; exclusive licensee American Association for the Advancement of Science. No claim to original U.S. Government Works

"Disruptor" residues in the regulator of G protein signaling (RGS) R12 subfamily attenuate the inactivation of Gα subunits

Ali Asli, Isra Sadiya, Meirav Avital-Shacham, Mickey Kosloff*

Understanding the molecular basis of interaction specificity between RGS (regulator of G protein signaling) proteins and heterotrimeric (αβγ) G proteins would enable the manipulation of RGS-G protein interactions, explore their functions, and effectively target them therapeutically. RGS proteins are classified into four subfamilies (R4, R7, RZ, and R12) and function as negative regulators of G protein signaling by inactivating Gα subunits. We found that the R12 subfamily members RGS10 and RGS14 had lower activity than most R4 subfamily members toward the G_i subfamily member $G\alpha_o$. Using structure-based energy calculations with multiple Gα-RGS complexes, we identified R12-specific residues in positions that are predicted to determine the divergent activity of this subfamily. This analysis predicted that these residues, which we call "disruptor residues," interact with the Gα helical domain. We engineered the R12 disruptor residues into the RGS domains of the high-activity R4 subfamily and found that these altered proteins exhibited reduced activity toward $G\alpha_o$. Reciprocally, replacing the putative disruptor residues in RGS18 (a member of the R4 subfamily that exhibited low activity toward $G\alpha_o$) with the corresponding residues from a high-activity R4 subfamily RGS protein increased its activity toward $G\alpha_o$. Furthermore, the high activity of the R4 subfamily toward $G\alpha_o$ was independent of the residues in the homologous positions to the R12 subfamily and RGS18 disruptor residues. Thus, our results suggest that the identified RGS disruptor residues function as negative design elements that attenuate RGS activity for specific Gα proteins.

INTRODUCTION

Heterotrimeric guanine nucleotide–binding proteins (G proteins) play a critical role in countless physiological processes, functioning as molecular switches in intracellular signal transduction pathways (*1*, *2*). The Gα subunit determines the activation state of the G protein switch, cycling between a guanosine diphosphate–bound inactive state and a guanosine 5′-triphosphate (GTP)–bound active state that mediates downstream signaling. The duration of heterotrimeric G protein signaling is controlled by RGS (regulator of G protein signaling) proteins that inactivate Gα subunits (*3*–*6*). This "turn off" function of RGS proteins is achieved by allosterically accelerating GTP hydrolysis in the Gα subunits. This allosteric regulation is mediated by the ~120–amino acid "RGS domain," which is present in all RGS proteins and is responsible for the function of RGS proteins as guanosine triphosphatase (GTPase)–activating proteins (GAPs) (*4*, *5*, *7*). As expected from their key role in G protein–coupled signaling, RGS proteins mediate numerous physiological functions, are involved in a wide range of human pathologies, and are considered promising drug targets (*8*–*12*).

Proteins with RGS domains represent a large and diverse family. Of these, the 20 "classical" or "canonical" RGS proteins can recognize and inactivate Gα subunits that belong to the G_i and G_q subfamilies. Canonical RGS proteins have been further divided into four subfamilies (R4, R7, RZ, and R12) based on their sequence similarity (*13*). The R4 subfamily is the largest, consisting of 10 members: RGS1, RGS2, RGS3, RGS4, RGS5, RGS8, RGS13, RGS16, RGS18, and RGS21 (*8*, *12*, *13*). With the noted exception of RGS2, which has no activity toward G_i subfamily members (*14*–*16*), members of the R4 subfamily are generally considered to have high GAP activity toward the G_i subfamily, with well-studied examples including RGS1 (*17*, *18*), RGS4 (*18*–*20*), and RGS16 (*18*, *21*–*23*). The R12 subfamily (RGS10, RGS12, and RGS14) is implicated in a range of physiological processes or pathologies. RGS10 is suggested to be involved in cardiovascular diseases (*24*), platelet function (*25*), macrophage activation (*26*), Parkinson's disease (*27*), and chemoresistance in ovarian cancer (*28*). RGS12 is implicated in neuron and bone differentiation (*29*, *30*), cardiac hypertrophy, and heart failure (*31*). RGS14 is abundant in the brain and is involved in spatial memory and learning (*32*, *33*), cell division and chemotaxis (*34*, *35*), and Parkinson's disease (*36*). Therefore, the R12 subfamily members attract considerable attention both as physiological modulators of signaling and as potential drug targets. However, their cellular targets and the exact role that their GAP function plays in these cascades are unknown.

Although R12 subfamily members were suggested to act as specific GAPs toward the G_i subfamily (*37*), previous studies reported different relative GAP activities for this subfamily. For example, the RGS10 RGS domain has high activity toward $G\alpha_i$ (*5*), and its GAP activity is higher toward $G\alpha_i$ and $G\alpha_z$ than is the activity of other RGS proteins, such as RGS19 and RGS4 (*38*). Compared to high-activity RGS proteins, such as RGS4 and RGS16, RGS12 (*39*, *40*) and RGS14 (*18*, *41*, *42*) exhibit lower GAP activity toward $G\alpha_i$. Other studies measured high GAP activity of RGS14 toward both $G\alpha_o$ and $G\alpha_i$ (*43*) or reported that RGS14 has a higher GAP activity than that of RGS4 toward $G\alpha_o$ and $G\alpha_i$ (*44*, *45*). Therefore, quantification of the GAP activities of this R12 subfamily in relation to those of R4 family members is lacking, as is an understanding of which amino acids determine R12 GAP activity toward the G_i subfamily.

The structural basis for the GAP activity and the selectivity of RGS domains is of great interest yet is only partially understood. To accelerate the GTPase activity of the Gα subunit, the RGS domain binds to the Gα-GTP complex and allosterically stabilizes the Gα catalytic machinery in its transition state conformation (*12*, *13*, *21*, *46*–*49*).

Department of Human Biology, Faculty of Natural Science, University of Haifa, Haifa 3498838, Israel.
*Corresponding author. Email: kosloff@sci.haifa.ac.il

Downloaded from http://stke.sciencemag.org/ on June 12, 2018

In all of the structures of Gα-RGS complexes solved to date, the RGS domain binds mainly to the GTPase domain of the Gα subunit (*16*, *37*, *46*, *50*–*53*). However, several of these structural studies report RGS interactions with another Gα domain, the Gα helical domain (*37*, *51*–*53*). In the G protein superfamily, the Gα helical domain is found only in the Gα subunits of heterotrimeric G proteins, and for many years, the purpose of the Gα helical domain was unclear. Suggested functional roles included increasing the affinity of the G protein for GTP (*54*), acting as an intrinsic GAP (*55*), or participating in effector recognition (*56*). The Gα helical domain is implicated in binding to inhibitory proteins, such as those with the GoLoco motif (*57*–*59*), and in catalyzing nucleotide exchange and Gα activation by G protein–coupled receptors (*60*). The previous structural studies of Gα-RGS complexes suggest that RGS contacts with the Gα helical domain are variable and heterogenic, properties consistent with this domain contributing to interaction specificity (*37*, *51*). Structural studies of RGS2 and RGS8 bound to $G\alpha_q$ also indicated that interactions with its Gα helical domain might play a role in dictating affinity or GAP "potency," the relative GTPase-accelerating activity of RGS proteins (*52*, *53*). Together, these studies raise two interconnected questions. First, are RGS domain interactions with the Gα helical domain functionally important for RGS GAP activity? Second, how might these interactions encode specificity among members of the RGS family?

In a previous study, we used energy calculations to analyze structures of RGS domains with Gα subunits from the G_i subfamily (*18*), identifying which RGS residues contribute substantially to interactions with these Gα subunits. We further classified these Gα-interacting RGS residues into two groups. The first group contains "Significant & Conserved" (S&C) residues, which make similar and substantial energy contributions across all available structures. These residues make most of the interactions with the residues adjacent to the Gα catalytic site and presumably have a primary role in accelerating Gα GTPase activity by stabilizing Gα in a conformation optimal for GTP hydrolysis (*1*, *12*, *49*, *61*). The second group contains "Modulatory" residues, which make substantial energy contributions only in some of the structures and are not conserved across all of the RGS domains. Modulatory residues are located at the periphery of the RGS domain interface with Gα subunits. We proposed that modulatory residues encode specific interactions with particular Gα subunits (*18*). Substitution of such modulatory residues in low-activity RGS proteins with their counterparts from high-activity RGS domains showed that these modulatory residues encode RGS selectivity in the RZ and R4 subfamilies. The hypothesis that emerged from this study is that RGS modulatory positions determine interaction specificity with Gα subunits. Yet, the mechanistic details of this putative role are lacking.

Here, we evaluated the relative GAP activities of R12 and R4 subfamily members toward the representative G_i subfamily member $G\alpha_o$. We found that, compared to the high-activity R4 subfamily members RGS4 and RGS16, the R12 subfamily members RGS10 and RGS14 had lower GAP activity toward $G\alpha_o$. Using structure-based computations, we identified R12-specific residues in modulatory positions that may be responsible for these differences in GAP activity. We analyzed these residues at the three-dimensional (3D) structural level and predicted that they interact with the Gα helical domain. We validated our computational predictions through mutagenesis of R4 and R12 RGS domains. Introducing the modulatory residues from R12 subfamily members into high-activity R4 subfamily members converted them into RGS proteins with low GAP activity toward $G\alpha_o$, whereas replacing the modulatory residues in R12 subfamily members with low GAP activity toward $G\alpha_o$ resulted in higher GAP activity toward this Gα subunit. Together, our results suggest that the R12-specific disruptor residues that we identified function as negative modulatory elements that attenuate RGS GAP activity in a specific fashion.

RESULTS

R12 subfamily members show lower GAP activity toward $G\alpha_o$ compared to that of high-activity RGS domains

We compared the GAP activities of RGS10 and RGS14, which are members of the R12 subfamily, with the activity of RGS16 and RGS4, which are representative members of the R4 subfamily with high activity toward the G_i subfamily (*18*, *20*, *21*, *23*, *62*). We used single-turnover GTPase assays with $G\alpha_o$ and a catalytic concentration of RGS proteins to calculate the catalytic rate (k_{GAP}) of the four RGS proteins according to previously published methodology (*48*, *63*, *64*). RGS10 and RGS14 had lower GAP activities toward $G\alpha_o$ (k_{GAP} = 0.5 and 0.3 min^{-1}, respectively), and RGS16 and RGS4 had higher GAP activities (k_{GAP} = 1.3 and 1.3 min^{-1}, respectively) (Fig. 1A). We also measured the GAP potency (*52*, *65*), the concentration of RGS protein that produced a 50% maximal increase in GTP hydrolysis [half-maximal effective concentration (EC_{50})], of RGS10, RGS14, and RGS16 (Fig. 1B). In this in vitro assay, RGS16 had a higher GAP potency than those of RGS10 and RGS14 (RGS16 EC_{50} = 7 nM; RGS10 EC_{50} = 42 nM; RGS14 EC_{50} = 63 nM). We then turned to energy-based analysis to identify which R12 residues might determine the lower GAP activities of these R12 subfamily members.

Energy calculations predict that R12-specific residues in modulatory positions perturb productive interactions with the Gα helical domain

On the basis of the methodology that we developed previously (*18*), we can use energy-based calculations to identify which RGS residues contribute substantially to interactions with Gα subunits. We analyzed four x-ray complexes of Gα subunits bound to three different RGS domains from R4 subfamily members with high GAP activity toward the G_i subfamily: RGS1, RGS4, and RGS16 (see Materials and Methods). Two of the complexes are of RGS16, which was solved in complexes with $G\alpha_i$ and $G\alpha_o$ (*37*, *51*). We used the

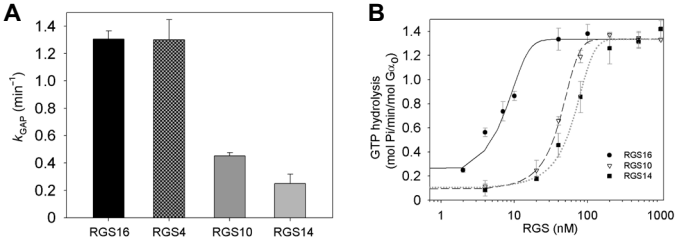

Fig. 1. RGS10 and RGS14 have lower GAP activities toward $G\alpha_o$ compared to those of RGS16 and RGS4. (**A**) k_{GAP} constants for RGS16, RGS4, RGS10, and RGS14 for GTP hydrolyzed by $G\alpha_o$ (400 nM) in the presence of RGS protein (20 nM). Data are means ± SEM of at least three independent biological replicates. (**B**) Dose-response analysis of RGS16, RGS10, and RGS14 activity toward $G\alpha_o$. The EC_{50} values (RGS16 = 7 ± 1 nM; RGS10 = 42 ± 2 nM; RGS14 = 63 ± 5 nM) were calculated using three-parameter sigmoidal curves. Data are means ± SEM of experiments performed in triplicate and are representative of three or more independent biological replicates for each RGS tested.

Downloaded from http://stke.sciencemag.org/ on June 12, 2018

finite-difference Poisson-Boltzmann (FDPB) method to calculate the net electrostatic and polar contributions ($\Delta\Delta G_{elec}$) of each RGS residue that is within 15 Å of the RGS-Gα interface in these complexes. Nonpolar energy contributions ($\Delta\Delta G_{np}$) were calculated as a surface-area proportional term by multiplying the per-residue surface area buried upon complex formation by a surface tension constant of 0.05 kcal/mol per Å^2. Our calculations indicated that electrostatic interactions represent most of the interactions between R4 RGS residues and $G\alpha_{i/o}$ (fig. S1). We classified RGS S&C and modulatory residues (*18*) and visualized them on the superimposed structures of these four complexes (Fig. 2A). Our analysis showed that RGS S&C residues interact only with the GTPase domain in all four structures. In contrast, we found that RGS modulatory residues interact both with the GTPase domain and with the Gα helical domain. Using the structures of $G\alpha_i$ with RGS16 (Fig. 2B) and RGS4 (Fig. 2C), we identified four modulatory residues in each RGS protein that interacted with the Gα helical domain. In RGS16, the modulatory residues Glu^{135}, Glu^{164}, Lys^{165}, and Lys^{173} contributed substantially to the interaction with the helical domain of the Gα subunit (Fig. 2B). In RGS4, Glu^{161}, Lys^{162}, Arg^{166}, and Lys^{170} contributed substantially to the interaction with the Gα helical domain (Fig. 2C). The RGS4 residues Glu^{161}, Lys^{162}, and Lys^{170} are equivalent to the RGS16 residues Glu^{164}, Lys^{165}, and Lys^{173}, respectively. Although there is no contributing RGS4 residue that corresponds to RGS16 Glu^{135}, Arg^{166}, which is unique to RGS4 among all classical RGS proteins (and corresponds to Pro^{169} in RGS16), contributed substantially to the interaction with the Gα helical domain.

To identify which R12 subfamily residues are responsible for the low GAP activity of these RGS proteins toward $G\alpha_o$, we mapped the results of our energy analysis onto the sequences of the representative R4 subfamily members and compared them to the sequences of the R12 RGS domains (Fig. 3). Using the available crystal structures of high-activity RGS proteins with $G\alpha_{i1}$ and $G\alpha_o$, we examined which substitutions of R4 residues in the R12 subfamily might hinder interactions with Gα subunits. Our analysis predicted that the contribution of all S&C residues is conserved across these R4 subfamily members (Fig. 3A) and across the three R12 subfamily members (Fig. 3B). Although most of the RGS modulatory residues were predicted to contribute similarly across the R12 subfamily and were thus classified as conserved modulatory residues (Fig. 3B), four modulatory positions were markedly different. Three of these residues, which we termed putative "disruptor" residues, are located in modulatory positions, are specific to the R12 subfamily, and were predicted to perturb the favorable interactions found in the R4 subfamily complexes with Gα subunits. In RGS16, these three modulatory positions (Glu^{135}, Glu^{164}, and Lys^{165}) interact with the Gα helical domain (Fig. 2B). The residues corresponding to RGS16 Glu^{164} and Lys^{165} are conserved in RGS4 and RGS1 (Fig. 3A). However, our structural analysis indicated that there is no contribution in RGS4 from Cys^{132} (Fig. 2C), which is the position that corresponds to RGS16 Glu^{135}. Rather, Arg^{166}, which is unique to RGS4, is predicted to contribute to interactions with the helical domain. We note that an arginine in this position is unique to RGS4 among all RGS family members. The last RGS modulatory position that, according to our calculations, interacts with the Gα helical domain (Lys^{173} in RGS16 and Lys^{170} in RGS4) is identical across the R4 and R12 subfamilies (Fig. 3) and is therefore not likely to contribute to their specificity toward Gα subunits.

Analyzing the structural differences between these R12 residues and the corresponding residues in high-activity R4 subfamily members suggested a mechanistic basis for the lower GAP activity of the R12 subfamily. We superimposed the structures of RGS16-$G\alpha_{i1}$ and RGS16-$G\alpha_o$ and visualized the modulatory RGS16 residues Glu^{135}, Glu^{164}, and Lys^{165} and their interacting partner residues in the Gα subunit (Fig. 4A). In the high-activity RGS16 protein, Lys^{165} forms an electrostatic and hydrogen bond network with multiple residues on both sides of the interface—an intramolecular salt bridge with RGS16 Glu^{164}, an intermolecular salt bridge with $G\alpha_{i1}$ Glu^{116} (located in the αB-αC loop), and a hydrogen bond with $G\alpha_{i1}$ Ser^{75} (Fig. 4A, top). We observed a similar interaction network in the complexes of $G\alpha_{i1}$ with RGS1 and RGS4 (fig. S2). One interaction that we observed in the structural analysis that was not predicted from the energy calculations was the electrostatic contributions of Lys^{165} to the interactions with $G\alpha_{i1}$. Because we calculated the energy difference between the monomers and the complex structures, which correspond to the

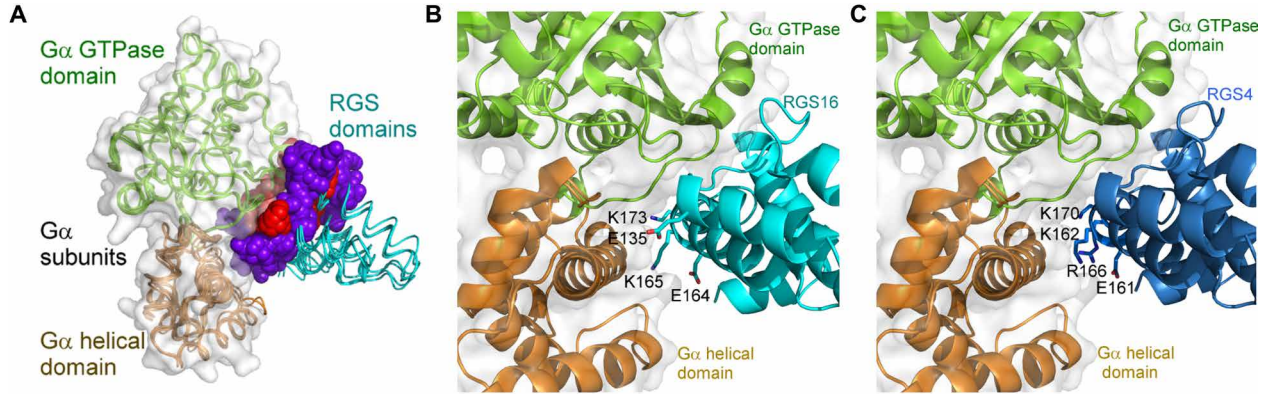

Fig. 2. RGS S&C residues interact with the Gα GTPase domain and RGS modulatory residues interact with the GTPase and helical domains of Gα. (**A**) Superimposition of four crystal structures of Gα-RGS complexes (with PDB codes): RGS1-$G\alpha_{i1}$ (PDB ID: 2GTP), RGS4-$G\alpha_{i1}$ (PDB ID: 1AGR), human RGS16–$G\alpha_{i1}$ (PDB ID: 2IK8), and mouse RGS16–$G\alpha_o$ (PDB ID: 3C7K). RGS domains (cyan) and Gα subunits (green and orange) are shown as backbone traces. $G\alpha_i$ in the RGS4-$G\alpha_{i1}$ structure is also visualized as a light gray transparent molecular surface. RGS S&C residues are shown as red spheres, and modulatory residues are shown as purple spheres. (**B**) Four RGS16 modulatory residues (Glu^{135}, Glu^{164}, Lys^{165}, and Lys^{173}, shown as sticks) interact with the helical domain of the Gα subunit. RGS and Gα subunits are shown as ribbon diagrams colored as in (A), rotated 20° about the *y* axis relative to (A). (**C**) Four RGS4 modulatory residues (Glu^{161}, Lys^{162}, Arg^{166}, and Lys^{170}; shown as sticks) interact with the helical domain of the Gα subunit, shown in the same orientation as in (B).

Downloaded from http://stke.sciencemag.org/ on June 12, 2018

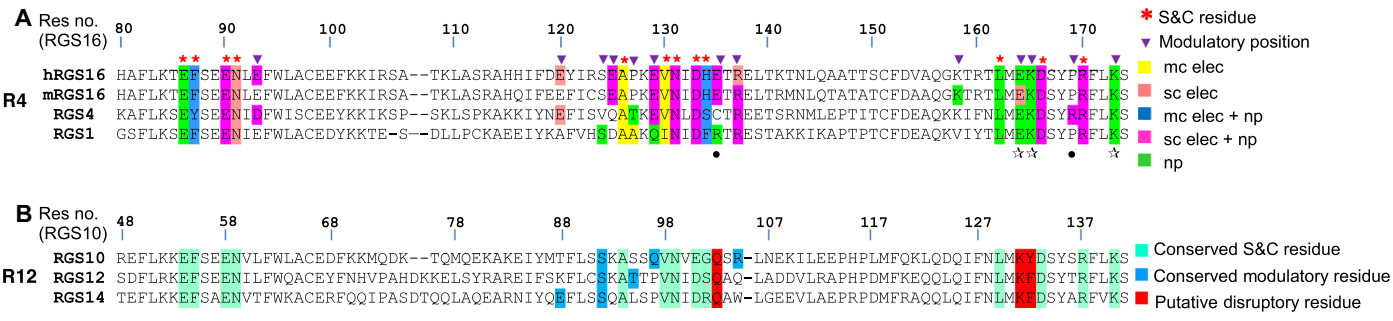

Fig. 3. R12 RGS residues in critical modulatory positions are predicted to disrupt intermolecular interactions with the Gα helical domain. (**A**) Residue-level sequence map summarizing our structure-based energy calculations of the R4 representative complexes with Gα subunits. Colored boxes mark RGS residues that contribute substantially to interactions with Gα subunits, according to the type of energy contribution: nonpolar (np), electrostatic (elec) contributions from the residue side chain (sc elec) or the main chain (mc elec). S&C residues for all four R4 structures are marked with red asterisks above the alignment, and modulatory positions that contribute in any of the four R4 structures are marked with purple triangles. An open star symbol marks modulatory RGS residues that contribute to interactions with the Gα helical domain across all of the analyzed high-activity R4 subfamily members; a black circle marks a contribution found only in some R4 high-activity representatives. The numbering above the alignment is according to the human RGS16 sequence. (**B**) Sequence-based prediction of R12 subfamily residue-level contributions, classified into three groups: Conserved S&C residues and conserved modulatory residues are residues that are identical across the relevant R4 and R12 subfamilies members; putative disruptor residues are R12-specific residues in modulatory positions that are different than their counterparts in the high-activity R4 subfamily and are predicted to impair the interaction with the Gα helical domain.

net electrostatic contributions to affinity in the complex, we interpreted the former result to mean that the Lys^{165}-mediated electrostatic network plays an allosteric role in RGS GAP activity rather than contributes to an increased RGS-Gα affinity. Moreover, the conformation of the αB-αC loop differs between $Gα_{i1}$ and $Gα_o$. Nevertheless, the corresponding residue to $Gα_{i1}$ Glu^{116} in $Gα_o$, Asp^{116}, forms a similar electrostatic interaction with RGS16 Lys^{165} (Fig. 4A, top).

Modeling the corresponding residues in RGS10 and RGS14 suggested that they perturb interactions with the Gα helical domain. We superimposed the structures of RGS10 and RGS14 on the structures of the RGS16-$Gα_{i1}$ and RGS16-$Gα_o$ complexes (Fig. 4B, top). This revealed that the KY (RGS10) and KF (RGS14) motifs cannot form the electrostatic and hydrogen-bond network found in the Gα complexes with high-activity RGS domains (Fig. 4B, top; see also Fig. 4A, top, and fig. S2). The third RGS16 modulatory residue, Glu^{135}, forms a salt bridge with Gα Arg^{90} (Fig. 4A, bottom). The corresponding residues in RGS10 (Gln^{103}) and RGS14 (Gln^{86}) cannot form such an intermolecular salt bridge (Fig. 4B, bottom). In $Gα_o$, the basic residue (Arg^{86}) that interacts with the RGS16 Glu^{135} originates one helix turn earlier than does Arg^{90} in $Gα_{i1}$. However, the guanidino groups of both basic Gα residues occupy essentially the same position and interact similarly with RGS16 Glu^{135}. The corresponding R12 glutamine residue is predicted to disrupt this interaction with both $Gα_{i1}$ and $Gα_o$ (Fig. 4B, bottom). The unique Arg^{166} residue in RGS4 forms a salt bridge with $Gα_{i1}$ Glu^{116} (Fig. 4C). The corresponding RGS10 Ser^{136} and RGS14 Ala^{119} residues cannot form such an intermolecular salt bridge (Fig. 4D). Together, these data suggest that the three putative disruptor residues in either RGS10 or RGS14 are predicted to have a similar negative effect on the interactions of these RGS domains with both $Gα_o$ and $Gα_{i1}$.

Looking across the R4 subfamily, we identified RGS18 as a unique member with putative disruptor residues in the same positions as the R12 putative disruptor residues. In the position that corresponds to RGS16 Lys^{165} (Fig. 4A), RGS18 has a glutamine (Gln^{186}). Similar to the R12 KY and KF motifs, Gln^{186} is predicted to perturb the electrostatic network with the Gα helical domain residues (Fig. 4E, left; see also Fig. 4B, top). In the position that corresponds to RGS16 Glu^{135} (Fig. 4A, bottom), RGS18 has a histidine (His^{156}) that, similar to the R12 residues in this position, cannot form an intermolecular salt bridge with the Gα helical domain residues (Fig. 4E, right). These results suggest that RGS18 contains the same putative disruptor elements as those of the R12 subfamily.

Inserting R12 putative disruptor residues into high-activity R4 subfamily members impairs their GAP activity

To examine whether the R12 putative disruptor residues that we identified are responsible for the lower GAP activities of RGS10 and RGS14, we inserted them into high-activity R4 subfamily members. We replaced all three or pairs of the corresponding RGS16 residues (Glu^{135}, Glu^{164}, and Lys^{165}) with their counterparts in RGS10 (Gln^{103}, Lys^{131}, and Tyr^{132}) or RGS14 (Gln^{86}, Lys^{114}, and Phe^{115}) and measured the GAP activities of these mutants using single-turnover GTPase assays. On the basis of our structural comparison (Fig. 4, A and B), we hypothesized that substituting the RGS16 Glu^{164}-Lys^{165} motif would have a more substantial effect on GAP activity than would substituting RGS16 Glu^{135} with the corresponding R12 glutamine motif. Substituting the RGS16 Glu^{164}-Lys^{165} motif with the RGS10 putative disruptor residues [to generate the RGS16 E164K-K165Y (EK>KY) mutant] reduced its GAP activity (Fig. 5A). The additional E135Q substitution (to generate the EEK>QKY mutant) did not further reduce GAP activity. When we substituted the RGS16 E164-K165 motif with the corresponding putative disruptor residues from RGS14, the RGS16 E164K-K165F (EK>KF) mutant exhibited a larger impairment in GAP activity than did the EK>KY mutant (Fig. 5A). The larger effect of the RGS14 disruptor residues, compared to that of the RGS10 residues, recapitulated the lower GAP activity of RGS14 compared to that of RGS10 (Fig. 1). In contrast with the EEK>QKY mutant, adding the E135Q mutation to the E164K-K165F mutant (EEK>QKF) further reduced GAP activity. As expected from the similarity of the disruptor motifs in the structures of RGS10, RGS14, and RGS18 (Fig. 4, B and E), substituting RGS16 Glu^{135} and Lys^{165} with their RGS18 putative disruptor counterparts (to generate the RGS16 mutant E135H-K165Q, E-K>H-Q)

Downloaded from http://stke.sciencemag.org/ on June 12, 2018

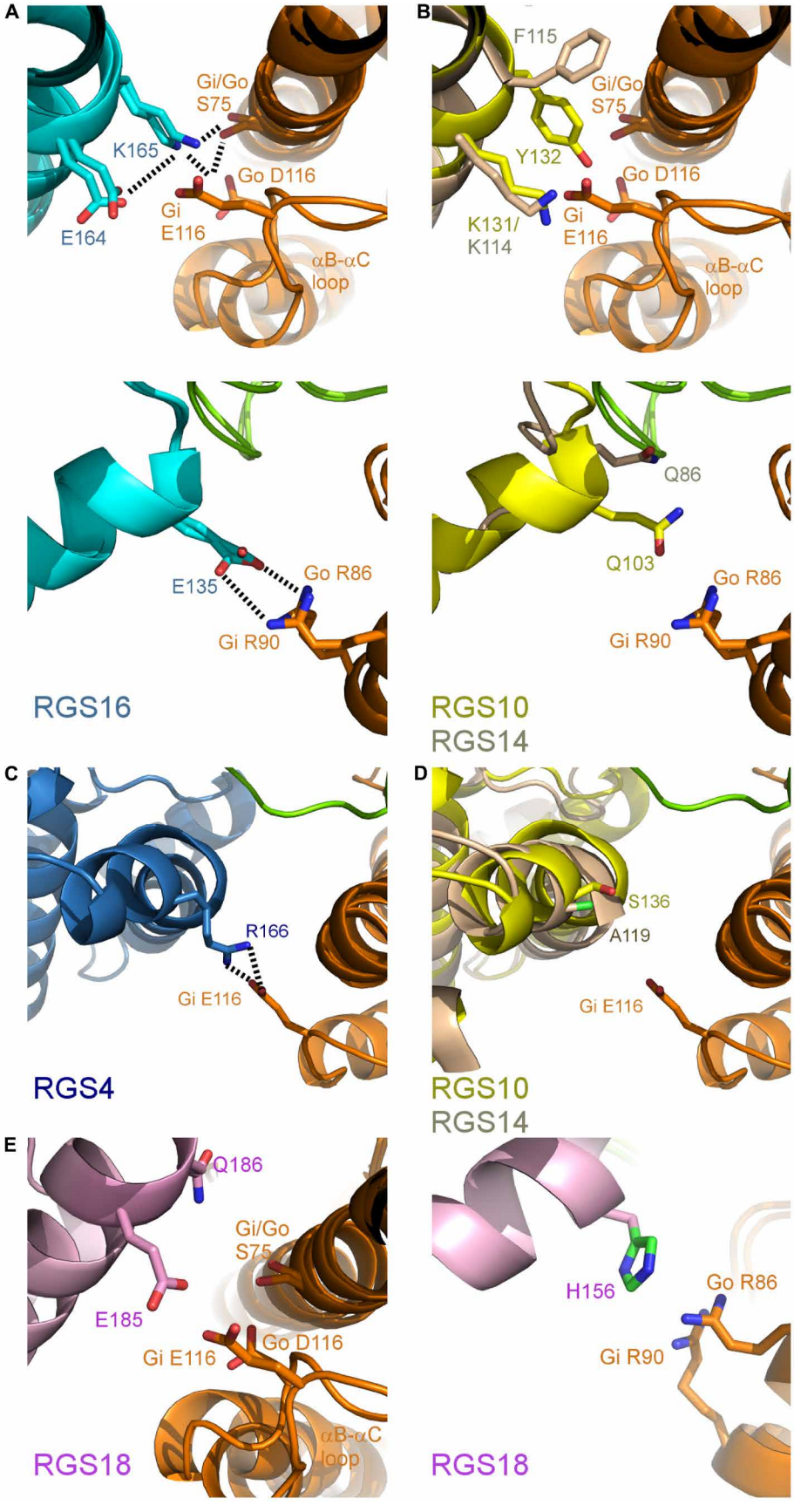

Fig. 4. Putative disruptor residues of RGS10, RGS14, and RGS18 are predicted to perturb favorable interactions with the helical domain of $G\alpha_{i/o}$. (**A**) RGS16 residues that contribute to favorable electrostatic interactions with the Gα helical domain, shown as sticks. Electrostatic interactions or hydrogen bonds are marked with dashed lines. The complexes of human RGS16–$G\alpha_{i1}$ and mouse RGS16–$G\alpha_o$ are superimposed and shown as ribbon diagrams: RGS16 (cyan) and Gα GTPase domain (green; bottom) and helical domain (orange; top and bottom). (**B**) Corresponding RGS10 and RGS14 putative disruptor residues, shown in stick form as in (A). RGS10 (yellow) and RGS14 (tan) were superimposed onto the complexes of human RGS16–$G\alpha_{i1}$ and mouse RGS16–$G\alpha_o$, with Gα colored as described in (A). (**C**) Electrostatic interaction between Arg^{166}, a unique modulatory residue in RGS4 (blue), and the $G\alpha_{i1}$ helical domain. (**D**) RGS10 (yellow) and RGS14 (tan) residues corresponding to RGS4-Arg^{166}, shown with the $G\alpha_{i1}$ helical domain residue that interacts with RGS4 Arg^{166}. (**E**) RGS18 (pink) putative disruptor residues (sticks), shown with the helical domain of $G\alpha_{i/o}$ with Gα colored as in (A). RGS18 was superimposed onto RGS16-$G\alpha_{i1}$ and RGS16-$G\alpha_o$, as described in (B).

also impaired GAP activity (Fig. 5A). In contrast, mutation of adjacent residues that were not predicted to contribute as much to the interaction between RGS16 and Gα, such as RGS16 residues (Tyr^{168} and Pro^{169} to Ala), did not impair GAP activity. Tyr^{168} is conserved across most RGS domains and is present in all high-activity R4 subfamily members and in all R12 subfamily members. Pro^{169} is conserved across all high-activity R4 subfamily members, with the exception of RGS4, in which the corresponding Arg^{166} is a unique contributing modulatory residue (Fig. 4C). In RGS14, the corresponding residue is an alanine (Fig. 4D). As expected from our energy calculations indicating that these two conserved residues do not contribute to interactions with Gα subunits (Fig. 3), the Y168A and the P169A mutants exhibited similar GAP activities to that of wild-type (WT) RGS16 (Fig. 5A).

In a reciprocal experiment, we replaced the RGS10 or the RGS14 putative disruptor residues with their RGS16 counterparts, which reduced GAP activity (fig. S3). The R12 subfamily has an adjacent heterogeneous structural region in the extended αV-to-αVI loop (*37*). We predict that this region will likely affect the local conformation of the R12 subfamily members. Therefore, we hypothesized that this heterogeneity does not enable substituted residues to reach the exact conformation seen in RGS16 or RGS4 (Fig. 4A and fig. S2). Thus, substituting only the two or three modulatory residues would be insufficient to

Downloaded from http://stke.sciencemag.org/ on June 12, 2018

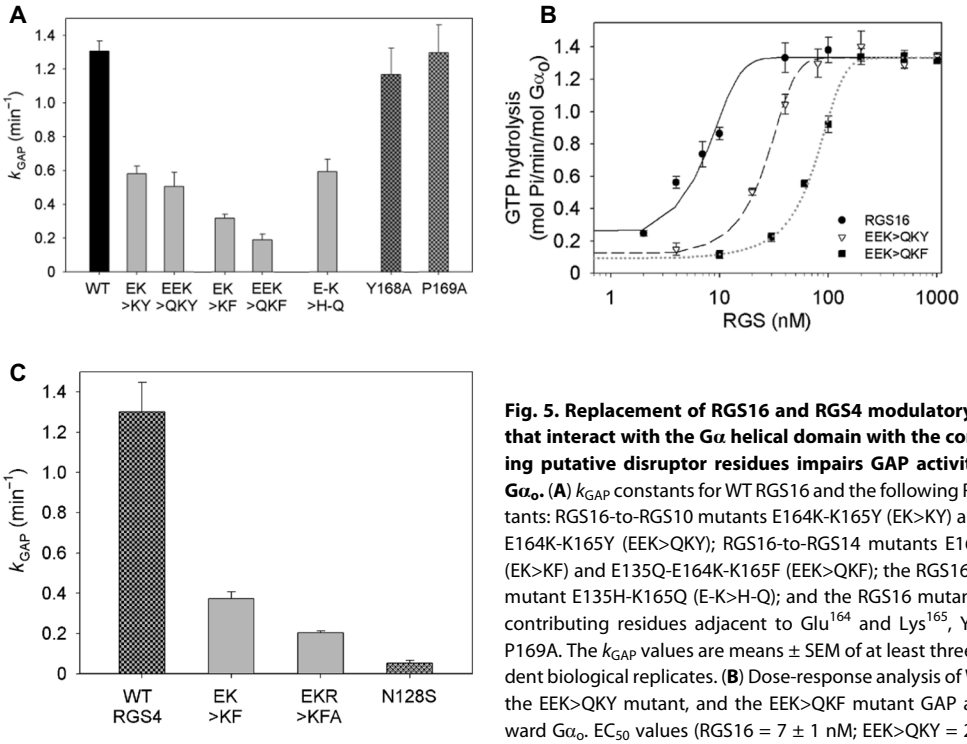

Fig. 5. Replacement of RGS16 and RGS4 modulatory residues that interact with the Gα helical domain with the corresponding putative disruptor residues impairs GAP activity toward Gα$_o$. (**A**) k_{GAP} constants for WT RGS16 and the following RGS16 mutants: RGS16-to-RGS10 mutants E164K-K165Y (EK>KY) and E135Q-E164K-K165Y (EEK>QKY); RGS16-to-RGS14 mutants E164K-K165F (EK>KF) and E135Q-E164K-K165F (EEK>QKF); the RGS16-to-RGS18 mutant E135H-K165Q (E-K>H-Q); and the RGS16 mutants in non-contributing residues adjacent to Glu^{164} and Lys^{165}, Y168A and P169A. The k_{GAP} values are means ± SEM of at least three independent biological replicates. (**B**) Dose-response analysis of WT RGS16, the EEK>QKY mutant, and the EEK>QKF mutant GAP activity toward Gα$_o$. EC_{50} values (RGS16 = 7 ± 1 nM; EEK>QKY = 26 ± 2 nM; EEK>QKF = 74 ± 3 nM) are means ± SEM of experiments performed in triplicate and are representative of at least three independent biological replicates each. (**C**) k_{GAP} constants for WT RGS4 and the following RGS4 mutants: RGS4-to-RGS14 mutants E161K-K162F and E161K-K162F-R166A and the RGS4 S&C residue mutant N128S. k_{GAP} values are means ± SEM of at least three independent biological replicates.

convert the RGS10 and RGS14 proteins into high-activity GAPs. However, an RGS14 chimera in which we substituted all RGS14 residues that can affect regions αV to αVI and αVII, which contain the three RGS14 disruptor residues Gln^{86}, Lys^{114}, and Phe^{115}, with their RGS16 counterparts, resulted in a protein with increased GAP activity compared to that of WT RGS14 (fig. S3).

Dose-response analysis of the GAP potencies of the RGS16 EEK>QKY and EEK>QKF mutants indicated that the GAP potency of these mutants was reduced (Fig. 5B). The EC_{50} of the EEK>QKY mutant was 26 nM, and the EC_{50} of the EEK>QKY mutant was 73 nM, whereas the EC_{50} of WT RGS16 was 7 nM (Fig. 5B). Therefore, these RGS16 mutants had a comparably reduced GAP potency, which was similar to that of RGS10 and RGS14. Similar to the RGS16 mutants, replacing the putative R12 subfamily disruptor residues in the corresponding positions of RGS4 reduced GAP activity (Fig. 5C). Substituting the RGS4 Glu^{161}-Lys^{162} motif, which corresponds to RGS16 Glu^{164}-Lys^{165}, with the corresponding RGS14 putative disruptor residues (to generate RGS4 E161K-K162F, the EK>KF mutant) substantially reduced GAP activity. Adding a substitution of the unique RGS4 Arg^{166} with its RGS14 counterpart to generate the triple mutant, RGS4 E161K-K162F-R166A (EKR>KFA), further reduced GAP activity. The k_{GAP} of this RGS4 triple mutant (0.2 min^{-1}) is similar to the k_{GAP} that we measured for WT RGS14 (0.3 min^{-1}; Fig. 1A). In comparison, mutating the RGS4 S&C residue Asn^{128}, which is essential for RGS catalytic activity (*18*, *21*, *48*), completely abolished RGS4 GAP activity (Fig. 5C).

To test whether RGS16 residues Glu^{135}, Glu^{164}, Lys^{165}, and Lys^{173}, which are the modulatory positions of RGS16 that interact with the Gα helical domain (Fig. 2B), are necessary for its high GAP activity, we mutated all four residues to alanines. The resulting RGS16-Ala$_4$ mutant had similar GAP activity to that of WT RGS16 (Fig. 6), suggesting that these residues are not essential for the high GAP activity of RGS16. This result indicates that alanines in these positions are permissible for high GAP activity; however, as we showed earlier, substituting the disruptor residues from low-activity RGS proteins, such as R12 family members, was not permissible for high GAP activity.

Replacing the putative RGS18 disruptor residues with their RGS16 counterparts increases GAP activity

To test whether substituting disruptor residues in the low-activity protein RGS18 with their high-activity RGS counterparts removes the negative effect on GAP activity, we replaced the RGS18 disruptor residues with their RGS16 counterparts (Fig. 7). The RGS18 Q186K mutant had increased GAP activity toward Gα$_o$. The RGS18 H156E-Q186K double mutant had further increased GAP activity, which was comparable to that of WT RGS16. Therefore, these data suggest that replacing these RGS18 disruptor residues with their RGS16 counterparts is sufficient for a complete gain of function.

DISCUSSION

The broad challenge of deciphering protein-protein interaction specificity is particularly relevant to the interactions of RGS proteins with Gα subunits. Because numerous RGS proteins are usually co-expressed in a given cell, identifying the molecular design principles that determine selective recognition of Gα subunits by RGS proteins is essential for understanding which RGS proteins mediate particular physiological functions and for manipulating these interactions with drugs. However, which RGS-Gα interactions occur and which residues encode the specificity of these interactions are mostly unclear, which is partially due to the low sequence identity among RGS domains (as low as 30%). Such low sequence identity increases the difficulty of pinpointing which residues contribute to similar interactions and which residues determine interaction selectivity. However, quantitative structure-based approaches, such as the approach we used here, can pinpoint which residues contribute substantially to interactions across a protein family and guide mutagenesis to redesign RGS interactions with Gα subunits.

Looking beyond the RGS family, specific protein-protein interactions between families of signaling proteins are crucial for the

Downloaded from http://stke.sciencemag.org/ on June 12, 2018

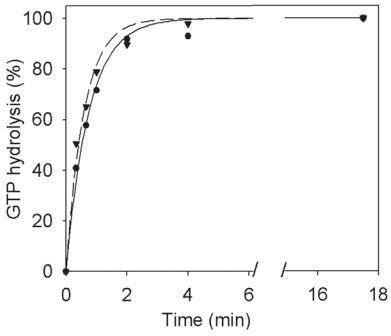

Fig. 6. Mutating all four RGS16 modulatory positions that interact with the Gα helical domain into alanines does not reduce the GAP activity of RGS16 toward $G\alpha_o$. Representative single-turnover GTPase assays of $G\alpha_o$ (400 nM) with RGS16 (20 nM; black circles and solid line) and the RGS16-Ala_4 mutant E135A-E164A-K165A-K173A (20 nM; black triangles and dashed line). The reaction rate constant (*k*) for RGS16 was 1.5 ± 0.3 min^{-1}, and that for the RGS16-Ala_4 mutant was 1.6 ± 0.2 min^{-1}. Data are means ± SEM of at least three independent biological replicates.

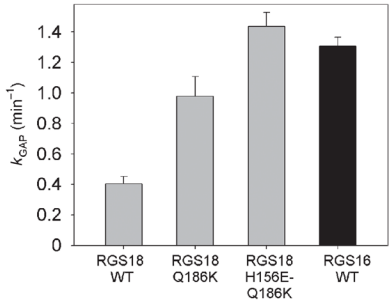

Fig. 7. Replacement of RGS18 disruptor residues with the corresponding RGS16 modulatory residues led to a gain of function. The k_{GAP} constants for WT RGS18, the RGS18-to-RGS16 mutants Q186K and H156E-Q186K, and WT RGS16 were calculated as in described in Fig.1. Data are means ± SEM of at least three independent biological replicates.

wiring of signaling networks. Useful terms to define structural elements that determine such specific interactions were coined by the protein design field: "Positive design elements" stabilize favorable interactions that strengthen particular protein pairings, whereas "Negative design elements" introduce unfavorable interactions that limit selected interactions between some family members (*66*, *67*). In particular, negative design elements are critical specificity determinants among well-studied examples in protein-protein interactions, such as heterodimeric coiled-coil pairs (*68*, *69*), colicin-immunity protein interactions (*70*, *71*), β-lactamase and its protein inhibitors (*72*), and Bcl-2 receptors binding to BH3-only proteins (*73*).

Previous studies identified RGS residues that are crucial positive design elements for RGS GAP function (*18*, *21*, *47*, *48*, *51*, *74*). We classified most of these previously studied RGS residues as S&C residues (Fig. 2A). These RGS residues interact with Gα residues adjacent to its catalytic site and presumably have a primary role in accelerating the GTPase activity of a Gα subunit by stabilizing a conformation that is optimal for GTP hydrolysis (*1*, *12*, *21*, *48*, *49*, *74*). However, to achieve high GAP activity, RGS domains also require sufficient modulatory residues that function as positive design elements. We had also suggested that modulatory residues encode specific interactions with particular Gα subunits (*18*).

Here, we found that R12 subfamily "disruptor residues" function as negative design elements by means of interacting with the Gα helical domain. Our results demonstrate that the R12 subfamily members RGS10 and RGS14 have reduced GAP activity toward $G\alpha_o$ compared to the high-activity RGS proteins, such as RGS4 and RGS16. Our structure-based analysis identified three R12 positions as critical for this phenotype. Mutating the corresponding RGS16 and RGS4 modulatory residues to their R12 counterparts reduced the GAP activities of RGS16 and RGS4 to those of RGS10 and RGS14. Because the S&C and modulatory residues of RGS12 are essentially identical to those of RGS14, and in particular, because their putative disruptor residues are identical, we suggest that these RGS domains will have similar GAP activity and specificity and that our results may be applicable to the entire R12 subfamily. Moreover, because mutating these residues in RGS16 to alanines did not reduce GAP activity, we conclude that these positions are not positive design elements in RGS16 but rather play a specific role as negative design elements in the R12 subfamily. Finally, we showed that replacing these negative design elements in RGS18 with their counterparts from RGS16 led to a complete gain of function, further supporting our conclusions that these negative design elements attenuate GAP activity through interactions with the Gα helical domain.

More generally, our energy calculations and structural analysis provide insights into how RGS domains encode specificity toward Gα subunits. Although it was known that RGS interactions with the Gα GTPase domain are central to RGS GAP activity (*1*, *21*, *48*, *49*) because the GTPase domain contains essentially all of the GTP-binding site, the functional roles of RGS interactions with the Gα helical domain were not clear. Our results show how contacts with the Gα helical domain can govern RGS-Gα interactions; a small number of key disruptor residues that interact with the Gα helical domain can fine-tune RGS GAP activity and determine specificity. Nevertheless, the interaction of these RGS modulatory residues with the Gα helical domain is not essential for high GAP activity, showing that these positions function as negative design elements only. Finally, the approach we used here can be leveraged to uncover additional positive and negative design elements across the larger RGS family and provide tools to rewire RGS interaction in cells and in vivo.

MATERIALS AND METHODS

Protein structures and sequences

We used the following 3D structures in our analysis and visualization of RGS-Gα complexes [with Protein Data Bank (PDB) codes for each structure]: rat RGS4–$G\alpha_{i1}$ (PDB ID: 1AGR) (*46*), human RGS16 (hRGS16)–$G\alpha_{i1}$ (PDB ID: 2IK8) (*37*), mouse RGS16 (mRGS16)–$G\alpha_o$ (PDB ID: 3C7K) (*51*), human RGS1–$G\alpha_{i1}$ (PDB ID: 2GTP) (*37*), human RGS10–$G\alpha_{i3}$ (PDB ID: 2IHB) (*37*), and the monomeric nuclear magnetic resonance (NMR) structures of human RGS14 (PDB ID: 2JNU) and RGS18 (PDB ID: 2JM5) (*37*). For visualization of the latter structures, we used the first model of the 20 NMR models in the PDB. 3D structural visualization and superimposition were performed with the molecular graphics program PyMOL (http://pymol.org). We used the following RGS domain sequences from the UniProt database (www.uniprot.org/): O43665 (RGS10), O14924 (RGS12), and O43566 (RGS14). Sequences were aligned using the T-Coffee server (http://tcoffee.vital-it.ch/apps/tcoffee/index.html), followed by manual adjustments in Jalview (www.jalview.org) according to our 3D structural comparisons.

Downloaded from http://stke.sciencemag.org/ on June 12, 2018

Energy calculations to identify RGS residues that contribute substantially to the RGS-Gα interactions

We followed a methodology described previously (*18*) to analyze the per-residue contributions of RGS residues to their Gα partner for the following crystal structures of RGS-Gα complexes (with PDB codes): human RGS16 (hRGS16)–$G\alpha_{i1}$ (PDB ID: 2IK8), mouse RGS16 (mRGS16)–$G\alpha_o$ (PDB ID: 3C7K), RGS4-$G\alpha_{i1}$ (PDB ID: 1AGR), and RGS1-$G\alpha_{i1}$ (PDB ID: 2GTP). We used the FDPB method to calculate the $\Delta\Delta G_{elec}$ of each residue that is within 15 Å of the dimer interface. Residues that contributed substantially to the interaction were defined as those contributing $\Delta\Delta G_{elec} \geq 1$ kcal/mol to the interactions (twice the numerical error of the electrostatic calculations) (*75*). $\Delta\Delta G_{np}$ were calculated as a surface-area proportional term by multiplying the per-residue surface area buried upon complex formation using surfv (*76*) by a surface tension constant of 0.05 kcal/mol per $Å^2$ (*75*). Residues that contributed substantially to binding were defined as those contributing $\Delta\Delta G_{np} \geq 0.5$ kcal/mol to the interactions (namely, bury more than 10 $Å^2$ of each protein surface upon complex formation).

Protein expression, purification, and mutagenesis

The RGS4, RGS10, RGS14, RGS16, and RGS18 domains were expressed in the pLIC-SGC1 vector as N-terminally His_6-tagged fusion proteins (Addgene). The N-terminally His_6-tagged rat $G\alpha_o$ clone was a gift from V. Arshavsky (Duke University). RGS16 mutants were generated with the QuikChange site-directed mutagenesis kit (Invitrogen) with primers designed using the Primer Design Program (www.genomics.agilent.com). An RGS14-to-RGS16 chimera was also generated with the QuikChange site-directed mutagenesis kit by inserting the mutations T29E, E30A, K34T, A38E, R103D, Q105A, A119P, and V122L and by replacing regions Gln^{76} to Pro^{80}, Arg^{85} to Asp^{101}, and Leu^{107} to Asn^{111} with their RGS16 counterparts. Proteins were expressed in *Escherichia coli* BL21 (DE3) cells and grown in 0.5 or 1 liter of LB broth at 37°C for RGS or Gα proteins, respectively, until OD_{600nm} (optical density at 600 nm) ≥ 1.4 was reached. The temperature was then reduced to 15°C, and protein expression was induced by addition of 0.5 mM or 100 μM isopropyl-D-thiogalactopyranoside for RGS or Gα proteins, respectively. After 16 to 18 hours, cells were harvested by centrifugation at 6000*g* for 30 min at 4°C, which was followed by freezing the pellets at −80°C. Bacterial pellets were suspended in lysis buffer [50 mM tris (pH 8.0), 50 mM NaCl, 5 mM $MgCl_2$, 5 mM β-mercaptoethanol, protease inhibitor cocktail (Roche), and 0.5 mM phenylmethylsulfonyl fluoride for G proteins only], and the cells were lysed with a Sonics Vibra-Cell sonicator, which was followed by centrifugation at 24,000*g* for 30 min at 4°C. The supernatants were equilibrated to 500 mM NaCl and 20 mM imidazole and loaded onto HisTrap FF 1-ml columns (GE Healthcare Life Sciences). The columns were washed with >20 volumes of wash buffer [20 mM tris (pH 8.0), 500 mM NaCl, and 20 mM imidazole] at 4°C, and the tagged proteins were eluted with elution buffer [20 mM tris (pH 8.0), 500 mM NaCl, and 100 mM imidazole (pH 8.0)]. The elute was loaded onto a HiLoad 16/600 Superdex 75 PG gel filtration column (GE Healthcare Life Sciences) at 4°C with ≥1.5 volumes of GF elution buffer [50 mM tris (pH 8.0), 50 mM NaCl, 5 mM β-mercaptoethanol, and 1 mM $MgCl_2$ added for Gα subunits only]. The eluate was dialyzed against a dialysis buffer [GF elution buffer with 40% (v/v) glycerol]. All purified proteins were estimated to be >95% pure, as assessed by SDS–polyacrylamide gel electrophoresis and Coomassie staining. Protein concentrations were determined by measuring their absorption at 280 nm using the predicted extinction coefficients (ProtParam, Swiss Institute for Bioinformatics) of the sequence of each expressed protein.

Single-turnover GTPase assays

Single-turnover GTPase assays using $G\alpha_o$ and the various RGS proteins were performed, as detailed in previous studies (*18*, *48*, *63*, *64*). Briefly, $G\alpha_o$ in reaction buffer [50 mM Hepes (pH 7.5), 0.05% (v/v) polyoxyethylene, 5 mM EDTA, bovine serum albumin (5 mg/ml), and 1 mM dithiothreitol] was incubated for 15 min at 20°C with 1 mM [γ-^{32}P]GTP and cooled on ice for 5 min. GTP hydrolysis was initiated by increasing the magnesium concentration to 5 mM (with $MgCl_2$), together with 100 μM cold GTP (final concentration) with or without RGS proteins at 4°C. Aliquots were taken at different time points and were quenched with 5% charcoal in 50 mM $Na_2H_2PO_4$ (pH 3) on ice, which was followed by centrifugation at 12,000*g* for 5 min at room temperature. The supernatant (200 μl) was transferred to 3 ml of liquid scintillation liquid (PerkinElmer) and analyzed with a Tri-Carb 2810 TR scintillation counter (PerkinElmer). GTPase rates were determined from single-exponential fits to the time courses using SigmaPlot 10.0. We calculated k_{GAP} rate constants by subtracting the basal GTPase rate (without RGS protein) from the GTPase rate that was measured in the presence of the RGS protein, as described previously (*64*).

RGS dose-response analysis

RGS dose-response analysis was performed as in previous studies (*52*, *65*). $G\alpha_o$ was loaded with 1 mM [γ-^{32}P]GTP for 15 min at 20°C in reaction buffer and then cooled on ice for 5 min. Each assay was initiated by adding 10 μl of RGS protein in different concentrations in assay buffer (5 mM $MgCl_2$ and 100 μM cold GTP) to a tube containing 20 μl of $G\alpha_o$ subunit (500 nM) on ice. Each reaction was terminated after 45 s by adding 100 μl of 5% perchloric acid and quenching with 700 μl of 10% (w/v) charcoal slurry in 50 mM phosphate buffer (pH 7.5), which was followed by centrifugation at 12,000*g* for 5 min at room temperature. The supernatant (200 μl) was transferred to 3 ml of liquid scintillation and analyzed with a Tri-Carb 2810 TR scintillation counter (PerkinElmer). EC_{50} values were determined from three-parameter sigmoidal curves with SigmaPlot 10.0.

SUPPLEMENTARY MATERIALS

www.sciencesignaling.org/cgi/content/full/11/534/eaan3677/DC1

Fig. S1. The RGS interface with Gα subunits is predominantly electrostatic and polar.

Fig. S2. A pair of RGS1 and RGS4 residues contributes favorably to electrostatic interactions with the Gα helical domain.

Fig. S3. A chimera of RGS14 and RGS16 exhibits increased GAP activity.

REFERENCES AND NOTES

1. S. R. Sprang, G protein mechanisms: Insights from structural analysis. *Annu. Rev. Biochem.* **66**, 639–678 (1997).
2. W. M. Oldham, H. E. Hamm, Heterotrimeric G protein activation by G-protein-coupled receptors. *Nat. Rev. Mol. Cell Biol.* **9**, 60–71 (2008).
3. M. R. Koelle, H. R. Horvitz, EGL-10 regulates G protein signaling in the C. elegans nervous system and shares a conserved domain with many mammalian proteins. *Cell* **84**, 115–125 (1996).
4. D. M. Berman, T. M. Wikie, A. G. Gilman, GAIP and RGS4 are GTPase-activating proteins for the Gi subfamily of G protein α subunits. *Cell* **86**, 445–452 (1996).
5. T. W. Hunt, T. A. Fields, P. J. Casey, E. G. Peralta, RGS10 is a selective activator of $G\alpha_i$ GTPase activity. *Nature* **383**, 175–177 (1996).
6. D. P. Siderovski, A. Hessel, S. Chung, T. W. Mak, M. Tyers, A new family of regulators of G-protein-coupled receptors? *Curr. Biol.* **6**, 211–212 (1996).

Downloaded from http://stke.sciencemag.org/ on June 12, 2018

7. N. Watson, M. E. Linder, K. M. Druey, J. H. Kehrl, K. J. Blumer, RGS family members: GTPase-activating proteins for heterotrimeric G-protein α-subunits. *Nature* **383**, 172–175 (1996).
8. S. Hollinger, J. R. Hepler, Cellular regulation of RGS proteins: Modulators and integrators of G protein signaling. *Pharmacol. Rev.* **54**, 527–559 (2002).
9. R. R. Neubig, D. P. Siderovski, Regulators of G-protein signalling as new central nervous system drug targets. *Nat. Rev. Drug Discov.* **1**, 187–197 (2002).
10. K. L. Neitzel, J. R. Hepler, Cellular mechanisms that determine selective RGS protein regulation of G protein-coupled receptor signaling. *Semin. Cell Dev. Biol.* **17**, 383–389 (2006).
11. J. H. Hurst, S. B. Hooks, Regulator of G-protein signaling (RGS) proteins in cancer biology. *Biochem. Pharmacol.* **78**, 1289–1297 (2009).
12. A. J. Kimple, D. E. Bosch, P. M. Giguère, D. P. Siderovski, Regulators of G-protein signaling and their Gα substrates: Promises and challenges in their use as drug discovery targets. *Pharmacol. Rev.* **63**, 728–749 (2011).
13. E. M. Ross, T. M. Wilkie, GTPase-activating proteins for heterotrimeric G proteins: Regulators of G protein signaling (RGS) and RGS-like proteins. *Annu. Rev. Biochem.* **69**, 795–827 (2000).
14. S. P. Heximer, N. Watson, M. E. Linder, K. J. Blumer, J. R. Hepler, RGS2/G0S8 is a selective inhibitor of Gqα function. *Proc. Natl. Acad. Sci. U.S.A.* **94**, 14389–14393 (1997).
15. S. P. Heximer, S. P. Srinivasa, L. S. Bernstein, J. L. Bernard, M. E. Linder, J. R. Hepler, K. J. Blumer, G protein selectivity is a determinant of RGS2 function. *J. Biol. Chem.* **274**, 34253–34259 (1999).
16. A. J. Kimple, M. Soundararajan, S. Q. Hutsell, A. K. Roos, D. J. Urban, V. Setola, B. R. S. Temple, B. L. Roth, S. Knapp, F. S. Willard, D. P. Siderovski, Structural determinants of G-protein α subunit selectivity by regulator of G-protein signaling 2 (RGS2). *J. Biol. Chem.* **284**, 19402–19411 (2009).
17. C. A. Johnston, J. P. Taylor, Y. Gao, A. J. Kimple, J. C. Grigston, J.-G. Chen, D. P. Siderovski, A. M. Jones, F. S. Willard, GTPase acceleration as the rate-limiting step in Arabidopsis G protein-coupled sugar signaling. *Proc. Natl. Acad. Sci. U.S.A.* **104**, 17317–17322 (2007).
18. M. Kosloff, A. M. Travis, D. E. Bosch, D. P. Siderovski, V. Y. Arshavsky, Integrating energy calculations with functional assays to decipher the specificity of G protein–RGS protein interactions. *Nat. Struct. Mol. Biol.* **18**, 846–853 (2011).
19. D. M. Berman, T. Kozasa, A. G. Gilman, The GTPase-activating protein RGS4 stabilizes the transition state for nucleotide hydrolysis. *J. Biol. Chem.* **271**, 27209–27212 (1996).
20. W. Cladman, P. Chidiac, Characterization and comparison of RGS2 and RGS4 as GTPase-activating proteins for m2 muscarinic receptor-stimulated G_i. *Mol. Pharmacol.* **62**, 654–659 (2002).
21. M. Natochin, R. L. McEntaffer, N. O. Artemyev, Mutational analysis of the Asn residue essential for RGS protein binding to G-proteins. *J. Biol. Chem.* **273**, 6731–6735 (1998).
22. T. Wieland, N. Bahtijari, X.-B. Zhou, C. Kleuss, M. I. Simon, Polarity exchange at the interface of regulators of G protein signaling with G protein α-subunits. *J. Biol. Chem.* **275**, 28500–28506 (2000).
23. A. Derrien, B. Zheng, J. L. Osterhout, Y.-C. Ma, G. Milligan, M. G. Farquhar, K. M. Druey, Src-mediated RGS16 tyrosine phosphorylation promotes RGS16 stability. *J. Biol. Chem.* **278**, 16107–16116 (2003).
24. S. D. Kim, H. J. Sung, S. K. Park, T. W. Kim, S. C. Park, S. K. Kim, J. Y. Cho, M. H. Rhee, The expression patterns of RGS transcripts in platelets. *Platelets* **17**, 493–497 (2006).
25. N. R. Hensch, Z. A. Karim, K. M. Druey, M. G. Tansey, F. T. Khasawneh, RGS10 negatively regulates platelet activation and thrombogenesis. *PLOS ONE* **11**, e0165984 (2016).
26. J.-K. Lee, J. Chung, G. T. Kannarkat, M. G. Tansey, Critical role of regulator G-protein signaling 10 (RGS10) in modulating macrophage M1/M2 activation. *PLOS ONE* **8**, e81785 (2013).
27. J.-K. Lee, J. Chung, F. E. McAlpine, M. G. Tansey, Regulator of G-protein signaling-10 negatively regulates NF-κB in microglia and neuroprotects dopaminergic neurons in hemiparkinsonian rats. *J. Neurosci.* **31**, 11879–11888 (2011).
28. S. B. Hooks, P. Callihan, M. K. Altman, J. H. Hurst, M. W. Ali, M. M. Murph, Regulators of G-protein signaling RGS10 and RGS17 regulate chemoresistance in ovarian cancer cells. *Mol. Cancer* **9**, 289 (2010).
29. M. D. Willard, F. S. Willard, X. Li, S. D. Cappell, W. D. Snider, D. P. Siderovski, Selective role for RGS12 as a Ras/Raf/MEK scaffold in nerve growth factor-mediated differentiation. *EMBO J.* **26**, 2029–2040 (2007).
30. X. Yuan, J. Cao, T. Liu, Y.-P. Li, F. Scannapieco, X. He, M. J. Oursler, X. Zhang, J. Vacher, C. Li, D. Olson, S. Yang, Regulators of G protein signaling 12 promotes osteoclastogenesis in bone remodeling and pathological bone loss. *Cell Death Differ.* **22**, 2046–2057 (2015).
31. J. Huang, L. Chen, Y. Yao, C. Tang, J. Ding, C. Fu, H. Li, G. Ma, Pivotal role of regulator of G-protein signaling 12 in pathological cardiac hypertrophy. *Hypertension* **67**, 1228–1236 (2016).
32. S. E. Lee, S. B. Simons, S. A. Heldt, M. Zhao, J. P. Schroeder, C. P. Vellano, D. P. Cowan, S. Ramineni, C. K. Yates, Y. Feng, Y. Smith, J. D. Sweatt, D. Weinshenker, K. J. Ressler, S. M. Dudek, J. R. Hepler, RGS14 is a natural suppressor of both synaptic plasticity in CA2 neurons and hippocampal-based learning and memory. *Proc. Natl. Acad. Sci. U.S.A.* **107**, 16994–16998 (2010).
33. M. F. López-Aranda, J. F. López-Téllez, I. Navarro-Lobato, M. Masmudi-Martín, A. Gutiérrez, Z. U. Khan, Role of layer 6 of V2 visual cortex in object-recognition memory. *Science* **325**, 87–89 (2009).
34. H. Cho, J. H. Kehrl, Localization of $G_{i\alpha}$ proteins in the centrosomes and at the midbody: Implication for their role in cell division. *J. Cell Biol.* **178**, 245–255 (2007).
35. L. Martin-McCaffrey, F. S. Willard, A. Pajak, L. Dagnino, D. P. Siderovski, S. J. A. D'Souza, RGS14 is a microtubule-associated protein. *Cell Cycle* **4**, 953–960 (2005).
36. I. R. Vogt, A. J. Lees, B. O. Evert, T. Klockgether, M. Bonin, U. Wüllner, Transcriptional changes in multiple system atrophy and Parkinson's disease putamen. *Exp. Neurol.* **199**, 465–478 (2006).
37. M. Soundararajan, F. S. Willard, A. J. Kimple, A. P. Turnbull, L. J. Ball, G. A. Schoch, C. Gileadi, O. Y. Fedorov, E. F. Dowler, V. A. Higman, S. Q. Hutsell, M. Sundström, D. A. Doyle, D. P. Siderovski, Structural diversity in the RGS domain and its interaction with heterotrimeric G protein α-subunits. *Proc. Natl. Acad. Sci. U.S.A.* **105**, 6457–6462 (2008).
38. S. Popov, K. Yu, T. Kozasa, T. M. Wilkie, The regulators of G protein signaling (RGS) domains of RGS4, RGS10, and GAIP retain GTPase activating protein activity in vitro. *Proc. Natl. Acad. Sci. U.S.A.* **94**, 7216–7220 (1997).
39. B. E. Snow, R. A. Hall, A. M. Krumins, G. M. Brothers, D. Bouchard, C. A. Brothers, S. Chung, J. Mangion, A. G. Gilman, R. J. Lefkowitz, D. P. Siderovski, GTPase activating specificity of RGS12 and binding specificity of an alternatively spliced PDZ (PSD-95/Dlg/ZO-1) domain. *J. Biol. Chem.* **273**, 17749–17755 (1998).
40. R. J. Kimple, L. De Vries, H. Tronchère, C. I. Behe, R. A. Morris, M. Gist Farquhar, D. P. Siderovski, RGS12 and RGS14 GoLoco motifs are $G\alpha_i$ interaction sites with guanine nucleotide dissociation inhibitor activity. *J. Biol. Chem.* **276**, 29275–29281 (2001).
41. J. R. Hepler, W. Cladman, S. Ramineni, S. Hollinger, P. Chidiac, Novel activity of RGS14 on Goα and Giα nucleotide binding and hydrolysis distinct from its RGS domain and GDI activity. *Biochemistry* **44**, 5495–5502 (2005).
42. P. Zhao, C. Nunn, S. Ramineni, J. R. Hepler, P. Chidiac, The Ras-binding domain region of RGS14 regulates its functional interactions with heterotrimeric G proteins. *J. Cell. Biochem.* **114**, 1414–1423 (2013).
43. S. Hollinger, J. B. Taylor, E. H. Goldman, J. R. Hepler, RGS14 is a bifunctional regulator of $G\alpha_{i/o}$ activity that exists in multiple populations in brain. *J. Neurochem.* **79**, 941–949 (2001).
44. S. Traver, C. Bidot, N. Spassky, T. Baltauss, M.-F. De Tand, J.-L. Thomas, B. Zalc, I. Janoueix-Lerosey, J. De Gunzburg, RGS14 is a novel Rap effector that preferentially regulates the GTPase activity of Gαo. *Biochem. J.* **350** pt. 1, 19–29 (2000).
45. H. Cho, T. Kozasa, K. Takekoshi, J. De Gunzburg, J. H. Kehrl, RGS14, a GTPase-activating protein for Giα, attenuates Giα- and G13α-mediated signaling pathways. *Mol. Pharmacol.* **58**, 569–576 (2000).
46. J. J. G. Tesmer, D. M. Berman, A. G. Gilman, S. R. Sprang, Structure of RGS4 bound to AlF_4^--activated $G_{i\alpha1}$: Stabilization of the transition state for GTP hydrolysis. *Cell* **89**, 251–261 (1997).
47. S. P. Srinivasa, N. Watson, M. C. Overton, K. J. Blumer, Mechanism of RGS4, a GTPase-activating protein for G protein α subunits. *J. Biol. Chem.* **273**, 1529–1533 (1998).
48. B. A. Posner, S. Mukhopadhyay, J. J. Tesmer, A. G. Gilman, E. M. Ross, Modulation of the affinity and selectivity of RGS protein interaction with G_α subunits by a conserved asparagine/serine residue. *Biochemistry* **38**, 7773–7779 (1999).
49. D. Mann, C. Teuber, S. A. Tennigkeit, G. Schroter, K. Gerwert, C. Kotting, Mechanism of the intrinsic arginine finger in heterotrimeric G proteins. *Proc. Natl. Acad. Sci. U.S.A.* **113**, E8041–E8050 (2016).
50. K. C. Slep, M. A. Kercher, W. He, C. W. Cowan, T. G. Wensel, P. B. Sigler, Structural determinants for regulation of phosphodiesterase by a G protein at 2.0 Å. *Nature* **409**, 1071–1077 (2001).
51. K. C. Slep, M. A. Kercher, T. Wieland, C.-K. Chen, M. I. Simon, P. B. Sigler, Molecular architecture of Gαo and the structural basis for RGS16-mediated deactivation. *Proc. Natl. Acad. Sci. U.S.A.* **105**, 6243–6248 (2008).
52. M. R. Nance, B. Kreutz, V. M. Tesmer, R. Sterne-Marr, T. Kozasa, J. J. G. Tesmer, Structural and functional analysis of the regulator of G protein signaling 2-$G\alpha_q$ complex. *Structure* **21**, 438–448 (2013).
53. V. G. Taylor, P. A. Bommarito, J. J. G. Tesmer, Structure of the regulator of G protein signaling 8 (RGS8)-$G\alpha_q$ complex: Molecular basis for Gα selectivity. *J. Biol. Chem.* **291**, 5138–5145 (2016).
54. J. P. Noel, H. E. Hamm, P. B. Sigler, The 2.2 Å crystal structure of transducin-α complexed with $GTP_\gamma S$. *Nature* **366**, 654–663 (1993).
55. D. W. Markby, R. Onrust, H. R. Bourne, Separate GTP binding and GTPase activating domains of a G alpha subunit. *Science* **262**, 1895–1901 (1993).
56. M. B. Mixon, E. Lee, D. E. Coleman, A. M. Berghuis, A. G. Gilman, S. R. Sprang, Tertiary and quaternary structural changes in $G_{i\alpha1}$ induced by GTP hydrolysis. *Science* **270**, 954–960 (1995).
57. R. J. Kimple, M. E. Kimple, L. Betts, J. Sondek, D. P. Siderovski, Structural determinants for GoLoco-induced inhibition of nucleotide release by Gα subunits. *Nature* **416**, 878–881 (2002).

Downloaded from http://stke.sciencemag.org/ on June 12, 2018

58. D. P. Siderovski, F. S. Willard, The GAPs, GEFs, and GDIs of heterotrimeric G-protein alpha subunits. *Int. J. Biol. Sci.* **1**, 51–66 (2005).
59. F. S. Willard, Z. Zheng, J. Guo, G. J. Digby, A. J. Kimple, J. M. Conley, C. A. Johnston, D. Bosch, M. D. Willard, V. J. Watts, N. A. Lambert, S. R. Ikeda, Q. Du, D. P. Siderovski, A point mutation to $G\alpha_i$ selectively blocks GoLoco motif binding: Direct evidence for Gα·GoLoco complexes in mitotic spindle dynamics. *J. Biol. Chem.* **283**, 36698–36710 (2008).
60. S. G. F. Rasmussen, B. T. DeVree, Y. Zou, A. C. Kruse, K. Y. Chung, T. S. Kobilka, F. S. Thian, P. S. Chae, E. Pardon, D. Calinski, J. M. Mathiesen, S. T. A. Shah, J. A. Lyons, M. Caffrey, S. H. Gellman, J. Steyaert, G. Skiniotis, W. I. Weis, R. K. Sunahara, B. K. Kobilka, Crystal structure of the β_2 adrenergic receptor–Gs protein complex. *Nature* **477**, 549–555 (2011).
61. Z. Chen, W. D. Singer, S. M. Danesh, P. C. Sternweis, S. R. Sprang, Recognition of the activated states of Gα13 by the rgRGS domain of PDZRhoGEF. *Structure* **16**, 1532–1543 (2008).
62. C.-K. Chen, T. Wieland, M. I. Simon, RGS-r, a retinal specific RGS protein, binds an intermediate conformation of transducin and enhances recycling. *Proc. Natl. Acad. Sci. U.S.A.* **93**, 12885–12889 (1996).
63. J. Wang, Y. Tu, J. Woodson, X. Song, E. M. Ross, A GTPase-activating protein for the G protein $G\alpha_z$. Identification, purification, and mechanism of action. *J. Biol. Chem.* **272**, 5732–5740 (1997).
64. E. M. Ross, Quantitative assays for GTPase-activating proteins. *Methods Enzymol.* **344**, 601–617 (2002).
65. S. Mukhopadhyay, E. M. Ross, Rapid GTP binding and hydrolysis by G_q promoted by receptor and GTPase-activating proteins. *Proc. Natl. Acad. Sci. U.S.A.* **96**, 9539–9544 (1999).
66. J. J. Havranek, P. B. Harbury, Automated design of specificity in molecular recognition. *Nat. Struct. Biol.* **10**, 45–52 (2003).
67. G. Schreiber, A. E. Keating, Protein binding specificity versus promiscuity. *Curr. Opin. Struct. Biol.* **21**, 50–61 (2011).
68. J. M. Mason, K. M. Müller, K. M. Arndt, Positive aspects of negative design: Simultaneous selection of specificity and interaction stability. *Biochemistry* **46**, 4804–4814 (2007).
69. A. W. Reinke, R. A. Grant, A. E. Keating, A synthetic coiled-coil interactome provides heterospecific modules for molecular engineering. *J. Am. Chem. Soc.* **132**, 6025–6031 (2010).
70. K. B. Levin, O. Dym, S. Albeck, S. Magdassi, A. H. Keeble, C. Kleanthous, D. S. Tawfik, Following evolutionary paths to protein-protein interactions with high affinity and selectivity. *Nat. Struct. Mol. Biol.* **16**, 1049–1055 (2009).
71. N. A. G. Meenan, A. Sharma, S. J. Fleishman, C. J. Macdonald, B. Morel, R. Boetzel, G. R. Moore, D. Baker, C. Kleanthous, The structural and energetic basis for high selectivity in a high-affinity protein-protein interaction. *Proc. Natl. Acad. Sci. U.S.A.* **107**, 10080–10085 (2010).
72. M. Gretes, D. C. Lim, L. de Castro, S. E. Jensen, S. G. Kang, K. J. Lee, N. C. J. Strynadka, Insights into positive and negative requirements for protein–protein interactions by crystallographic analysis of the β-lactamase inhibitory proteins BLIP, BLIP-I, and BLP. *J. Mol. Biol.* **389**, 289–305 (2009).
73. S. Dutta, S. Gullá, T. S. Chen, E. Fire, R. A. Grant, A. E. Keating, Determinants of BH3 binding specificity for Mcl-1 *versus* Bcl-x_L. *J. Mol. Biol.* **398**, 747–762 (2010).
74. S. R. Sprang, Z. Chen, X. Du, Structural basis of effector regulation and signal termination in heterotrimeric Gα proteins. *Adv. Protein Chem.* **74**, 1–65 (2007).
75. F. B. Sheinerman, B. Al-Lazikani, B. Honig, Sequence, structure and energetic determinants of phosphopeptide selectivity of SH2 domains. *J. Mol. Biol.* **334**, 823–841 (2003).
76. S. Sridharan, A. Nicholls, B. Honig, A new vertex algorithm to calculate solvent accessible surface-areas. *FASEB J.* **6**, A174 (1992).

Acknowledgments: We thank L. Barki-Harrington, E. Privman, and E. D. Levy for helpful comments and V. Arshavsky for the $G\alpha_o$ clone. **Funding:** This work was supported by grants from the Israel Science Foundation (grant numbers 1454/13, 1959/13, and 2155/15), the Israel Ministry of Science, Technology and Space, Israel, and the Italian Ministry of Foreign Affairs (3-10704). The authors acknowledge the contribution of COST Action CM-1207 (GLISTEN) to this work. **Author contributions:** A.A. designed the research, conducted most of the experiments and structural analysis, analyzed the results, and wrote the manuscript. I.S. conducted structural analysis and some of the experiments and analyzed the results. M.A.-S. conducted experiments, supervised the laboratory work, and analyzed the results. M.K. designed and supervised the research and wrote the manuscript. All authors were involved in the writing of the manuscript and approved the final version. **Competing interests:** The authors declare that they have no competing interests. **Data and materials availability:** Plasmids require a material transfer agreement from Addgene. All data needed to evaluate the conclusions in the paper are present in the paper or the Supplementary Materials.

Submitted 3 April 2017
Accepted 25 May 2018
Published 12 June 2018
10.1126/scisignal.aan3677

Citation: A. Asli, I. Sadiya, M. Avital-Shacham, M. Kosloff, "Disruptor" residues in the regulator of G protein signaling (RGS) R12 subfamily attenuate the inactivation of Gα subunits. *Sci. Signal.* **11**, eaan3677 (2018).

Downloaded from http://stke.sciencemag.org/ on June 12, 2018

Science Signaling

"Disruptor" residues in the regulator of G protein signaling (RGS) R12 subfamily attenuate the inactivation of G α subunits

Ali Asli, Isra Sadiya, Meirav Avital-Shacham and Mickey Kosloff

Sci. Signal. **11** (534), eaan3677.
DOI: 10.1126/scisignal.aan3677

Designing specificity

Once an agonist binds to its G protein–coupled receptor, GTP replaces GDP on the α subunit of an associated G protein, which then dissociates from its βγ dimer to activate effectors. The GTPase activity of the α subunit returns the G protein to an inactive state, a process that is accelerated by interactions with members of the regulator of G protein signaling (RGS) family. Asli *et al*. used functional and structural analyses to identify specific amino acid residues that distinguished RGS proteins with low activity toward G α_o from those with high activity. High-activity RGS proteins that were mutated to contain these "disruptor" residues exhibited reduced inhibitory activity toward the G α subunit. Together, these data suggest that "disruptor" residues within RGS proteins may encode specificity toward G α subunits.

ARTICLE TOOLS http://stke.sciencemag.org/content/11/534/eaan3677

SUPPLEMENTARY MATERIALS http://stke.sciencemag.org/content/suppl/2018/06/08/11.534.eaan3677.DC1

RELATED CONTENT
http://stke.sciencemag.org/content/sigtrans/9/420/ra30.full
http://stke.sciencemag.org/content/sigtrans/9/423/ra37.full
http://stke.sciencemag.org/content/sigtrans/11/519/eaao4220.full

REFERENCES This article cites 76 articles, 33 of which you can access for free
http://stke.sciencemag.org/content/11/534/eaan3677#BIBL

PERMISSIONS http://www.sciencemag.org/help/reprints-and-permissions

Use of this article is subject to the Terms of Service

Science Signaling (ISSN 1937-9145) is published by the American Association for the Advancement of Science, 1200 New York Avenue NW, Washington, DC 20005. 2017 © The Authors, some rights reserved; exclusive licensee American Association for the Advancement of Science. No claim to original U.S. Government Works. The title *Science Signaling* is a registered trademark of AAAS.

Downloaded from http://stke.sciencemag.org/ on June 12, 2018

Science Signaling
AAAS

www.sciencesignaling.org/cgi/content/full/11/534/eaan3677/DC1

Supplementary Materials for

"Disruptor" residues in the regulator of G protein signaling (RGS) R12 subfamily attenuate the inactivation of Gα subunits

Ali Asli, Isra Sadiya, Meirav Avital-Shacham, Mickey Kosloff*

*Corresponding author. Email: kosloff@sci.haifa.ac.il

Published 12 June 2018, *Sci. Signal.* **11**, eaan3677 (2018)
DOI: 10.1126/scisignal.aan3677

This PDF file includes:

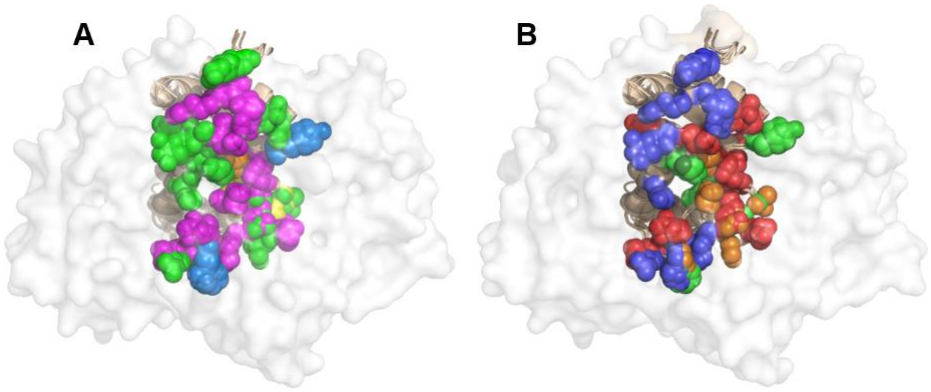

Fig. S1. The RGS interface with Gα subunits is predominantly electrostatic and polar. (**A** and **B**) R4 RGS residues that contribute predominantly to the interaction with Gα subunits are shown as spheres. (A) R4 RGS residues are colored by the type of their energy contribution as follows: nonpolar (green), main-chain electrostatic (yellow), side-chain electrostatic (orange), main-chain electrostatic and nonpolar (light blue), side-chain electrostatic and nonpolar (magenta). The four representative structures of the high-activity R4 subfamily are superimposed with RGS domains shown as ribbon diagrams (wheat) viewed through the transparent surface of the $G\alpha_{i1}$ subunit. (B) residues are colored according to their R4 RGS physicochemical properties as follows: basic residues (dark blue), acidic residues (red), polar residues (orange), all other residues (green).

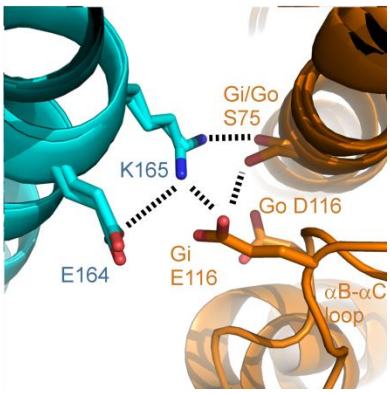

Fig. S2. A pair of RGS1 and RGS4 residues contributes favorably to electrostatic interactions with the Gα helical domain. The complexes of RGS1-Gα_{i1} and RGS4-Gα_{i1} were superimposed on the structures of human RGS16–Gα_{i1} and mouse RGS16–Gα_{o}. The RGS domains of RGS1 and RGS4 (cyan) and Gα subunits (orange and brown) are shown as ribbon diagrams. The Gα helical domain is orange. Contributing residues are shown as sticks, and favorable electrostatic interactions and hydrogen bonds are marked with dashed lines. For only the RGS16 interactions with Gα, see Fig. 4A.

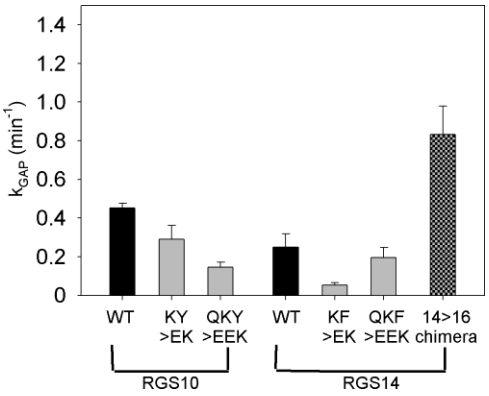

Fig. S3. A chimera of RGS14 and RGS16 exhibits increased GAP activity. k_{GAP} constants for WT RGS10, WT RGS14, and the following mutants: RGS10-to-RGS16 mutants K131E-Y132K (KY>EK) and Q103E-K131E-Y132K (QKY>EEK); RGS14-to-RGS16 mutants K114E-F115E (KF>EK) and Q86E-K114E-F115K (QKF>EEK); RGS14-to-RGS16 chimera (14>16 chimera) with the following replacements: T29E, E30A, K34T, A38E, Gln^{76} to Pro^{80}, Arg^{85} to Asp^{101}, R103D, Q105A, Leu^{107} to Asn^{111}, A119P, V122L. In this chimera, all RGS14 residues that can affect regions αV to αVI and αVII, which include the RGS14 disruptor residues Gln^{86}, Lys^{114}, Phe^{115}, were substituted with their RGS16 counterparts. The k_{GAP} constants were calculated as described in Fig. 1. Data are means ± SEM of at least three independent biological replicates.